——, and C. J. Powell, 1980: Vertical wavenumber spectra of temperature finestructure in the Equatorial Pacific. *J. Geophys. Res.*, **85**, 4029–4035.

Horne, E. P. W., 1978: Interleaving at the subsurface front in the Slope Water off Nova Scotia. *J. Geophys. Res.*, **83**, 3659–3671.

Joyce, T. M., 1977: A note on the lateral mixing of water masses. *J. Phys. Oceanogr.*, **7**, 626–629.

——, W. Zenk and J. M. Toole, 1978: The anatomy of the Antarctic Polar Front in the Drake Passage. *J. Geophys. Res.*, **83**, 6093–6113.

Mangum, L. J., N. N. Soreide, B. D. Davies, B. D. Spell and S. P. Hayes, 1980: CTD/O_2 measurements during the Equatorial Pacific Ocean Climate Studies (EPOCS) in 1979. NOAA Data Rep., ERL PMEL-1, 645 pp.

Pingree, R. D., 1971: Analysis of the temperature and salinity small-scale structure in the region of Mediterranean influence in the N.E. Atlantic. *Deep-Sea Res.*, **18**, 485–491.

Ruddick, B. R., and J. S. Turner, 1979: The vertical length scale of double-diffusive intrusions. *Deep-Sea Res.*, **26**, 903–913.

Stern, M. E., 1967: Lateral mixing of water masses. *Deep-Sea Res.*, **14**, 747–753.

Toole, J. M., 1981: Intrusion characteristics in the Antarctic Polar Front. *J. Phys. Oceanogr.*, **11**, 780–793.

——, and D. T. Georgi, 1981: On the dynamics and effects of double-diffusively driven intrusions. *Prog. Oceanogr.*, **10** (in press).

Alternative Parameterizations of Downward Irradiance and Their Dynamical Significance

J. J. SIMPSON

Scripps Institution of Oceanography, La Jolla, CA 92093

T. D. DICKEY

Institute for Marine and Coastal Studies and Department of Geological Sciences, University of Southern California, Los Angeles 90007

18 December 1980 and 1 March 1981

ABSTRACT

The effect of solar flux divergence on upper ocean dynamics and energetics under both low and high wind speeds was determined using four different parameterizations of downward irradiance. The first (case I) involved only one attenuation length, the second (case II) involved two attenuation lengths, the third (case III) used a spectral decomposition of the incident solar flux over nine wavelength bands, and the fourth (case IV) used an arctangent model of downward irradiance. The Mellor-Yamada turbulence closure scheme (level 2½) was used for the simulations. Cases II–IV predict the existence of an intensified shallow shear zone which is consonant with recent observations. At low wind speeds, the turbulent energy budget is dominated by shear production, dissipation and the diffusion of turbulent kinetic energy, regardless of parameterization. At high wind speeds, shear production is balanced by dissipation. Specific recommendations are made for parameterizing the downward irradiance in the context of numerical studies of upper ocean dynamics, general circulation and climate studies.

1. Introduction

Physical processes which occur at the air-sea interface and within the mixed layer and thermocline are critically dependent on the vertical distribution of downward irradiance within the upper ocean. Models of upper ocean dynamics [see reviews by Kraus (1977) and by Garwood (1979)] make various assumptions about the vertical distribution of downward irradiance. These assumptions are known (e.g., Kraus and Turner, 1967; Denman, 1973; Alexander and Kim, 1976; Kondo *et al.*, 1979) to affect the predicted thermal and density structure. More recently, Simpson and Dickey (1981) have shown that for low wind speeds ($U_{10} \leq 10$ m s^{-1}) significantly different dynamics and energetics occur within the mixed layer for two different parameterizations of downward irradiance. Dickey and Simpson (1981) have shown that diurnal changes in the heat content of the upper ocean are affected strongly by the particular parameterization used to model the divergence of downward irradiance. These latter results may have implications for climate studies. In addition, biological and chemical processes (e.g., photosynthesis and the solubility of dissolved gases in seawater) are influenced by the divergence of downward irradiance.

This note evaluates the effects of the divergence of downward irradiance on upper ocean dynamics and energetics under both low and high wind forcing conditions using four different parameterizations of downward irradiance. Specific recommendations, influenced by some likely oceanographic applica-

0022-3670/81/060876-07$05.75

tions, are made for choosing the most appropriate parameterization.

2. Downward irradiance

For optically homogeneous water, the vertical distribution of downward irradiance is given by

$$I(z) = \int_{\lambda=0}^{\infty} I(\lambda, z)d\lambda = \int_{z=0}^{z}\int_{\lambda=0}^{\infty} I(\lambda, 0)\exp[z/\zeta(\lambda)]d\lambda dz, \quad (1)$$

where $I(\lambda, z)$ is the irradiance per unit wavelength for wavelength λ at depth z, $\zeta(\lambda)$ the irradiance attenuation length for wavelength λ and z the vertical coordinate positive upward with origin at mean sea level.

The most frequently used (Tyler and Preisendorfer, 1962; Denman, 1973; Jerlov, 1976; Haney and Davies, 1976; Alexander and Kim, 1976) approximation to (1) is

$$I(z) = I_0 \exp(z/\zeta_1), \quad (2)$$

where $I(z)$, the downward irradiance, is the radiant flux density on a horizontal surface due to contributions from the entire upward hemisphere, I_0 the incident less reflected and emergent irradiance at the surface, and ζ_1 the attenuation length, assumed constant with depth. Several authors (Sverdrup *et al.*, 1942; Kondo and Watabe, 1969; Paulson and Simpson, 1977; Zaneveld and Spinrad, 1980) have shown that (2) is a poor approximation to (1) in the upper 10 m of the ocean because of the preferential absorption of the short- and longwave components of light. However, below a depth of 10 m, (2) is a good approximation because wavelength-dependent absorption has left only blue-green light. A better approximation to (1) is the bi-modal exponential parameterization suggested by Kraus (1972) and by Paulson and Simpson (1977)

$$I(z) = I_0\{R\exp(z/\zeta_1) + (1 - R)\exp(z/\zeta_2)\}. \quad (3)$$

The first term in (3) characterizes the rapid attenuation in the upper 5 m due to absorption of red spectral components while absorption of the blue-green spectral components below a depth of 10 m is characterized by the second term (i.e., $\zeta_2 > \zeta_1$). Absorption of the ultraviolet in the near surface layer is not explicitly included in (3) because the heat contribution in the ultraviolet region is relatively small compared to that in the red region of the spectrum. Perhaps the best approximation to (1) is the spectral decomposition of the downward irradiance into many wavelength bands,

$$I(z) = I_0 \sum_{i=1}^{n} a_i \exp(z/\zeta_i), \quad (4)$$

where n is the number of wavelength bands and the a_i and ζ_i are irradiance constants analogous to the set (R, ζ_1, ζ_2) used with (3). Values of these constants were calculated from the data given by Defant (1961). Vertical profiles of the downward irradiance within these wavelength bands are shown in Fig. 1. The red spectral components within the range 0.9 μm $\leq \lambda \leq$ 3.0 μm are all strongly attenuated within the first few tens of centimeters of the sea surface. Blue-green light penetrates much deeper. The total downward irradiance I(z) obtained from (4) is not as smooth a curve as those obtained from (2) and (3). This results from the coarse resolution in $d\lambda$ over which the measurements were made and experimental uncertainties in the measurements. However, these effects are shown below to have little or no effect on the simulations. Zaneveld and Spinrad (1980) have suggested an arctangent approximation to (1), i.e.,

$$I(z) = I_0 \exp(z/\zeta_2)[1 - R\tan^{-1}(-z/\zeta_1)], \quad (5)$$

where ζ_1 and ζ_2 are attenuation lengths and R is a partition function analogous to the R in (3). This expression, like (3), determines the profile of downward irradiance from three empirical constants. However, the longwave components of the solar spectrum are more strongly attenuated with (5) than with (3). The irradiance constants ζ_1, ζ_2 and R used with (5) correspond to the set K_3, K_1 and K_2 reported by Zaneveld and Spinrad (1980).

Values of the irradiance constants for type I open-ocean water (Jerlov, 1976) for the above parameterizations of downward irradiance are given in Table 1. Vertical profiles of downward irradiance corresponding to Eqs. (2)–(5) are given in Fig. 2. Differences in these profiles suggest that both the dynamics and energetics of the upper ocean are influenced by the choice of parameterization and that the choice must be consonant with the particular physical processes under study and their associated length scales (e.g., mixed-layer dynamics, thermal boundary layers, photosynthesis, gas exchange dynamics).

3. Analysis and discussion

The level 2½ version of the Mellor-Yamada (1974) turbulence closure scheme (e.g., Yamada, 1977; Blumberg and Mellor, 1980; Simpson and Dickey, 1981) was chosen for the present study because of its capacity to distribute downward irradiance differentially with depth rather than in an integrated fashion as would be required by an integral model. The conservation of heat equation differs from that used by Mellor and Durbin (1975) and by Blumberg and Mellor (1980) because the divergence of the downward irradiance is included. This equation may be written in the form

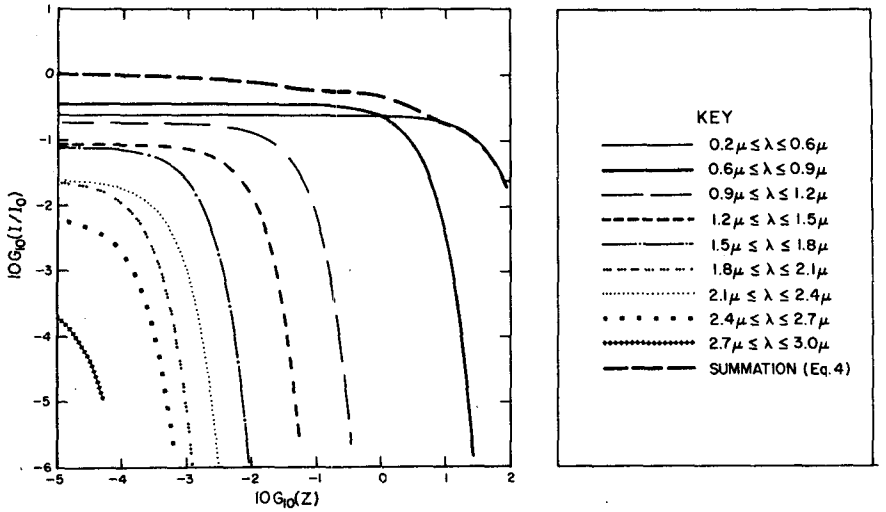

FIG. 1. Vertical profiles of the spectrally decomposed normalized downward irradiance for type I water [i.e., Eq. (4)].

$$\rho c_p \frac{\partial T}{\partial t} + \rho c_p \frac{\partial}{\partial z} \overline{w'T'} = Q(z) = \frac{\partial I}{\partial z}, \qquad (6)$$

where T is the mean temperature, ρ the *in situ* density and c_p the specific heat of sea water. The first term is the local rate of change of heat, the second term is the vertical divergence of the turbulent heat flux, and the right-hand side of (6) is the vertical divergence of the downward irradiance flux. The level 2½ version was used for these calculations because it includes the diffusion of turbulent kinetic energy in the local energy balance. This term appears to be important for low wind speeds (Simpson and Dickey, 1981). The vertical grid spacing was

TABLE 1. Alternative parameterizations of downward irradiance for type I open ocean water.

Case	R	ζ_1 (m)	ζ_2 (m)
I [Eq. (2)]			
Single exponential: $I(z) = I_0 \exp(z/\zeta_1)$			
Typically used (Denman, 1973; Alexander and Kim, 1976)	—	10	—
II [Eq. (3)]			
Double exponential: $I(z) = I_0[R \exp(z/\zeta_1) + (1 - R) \exp(z/\zeta_2)]$			
Paulson and Simpson (1977)	0.580	0.35	23
III [Eq. (4)]			
Spectral decomposition: $I(z) = I_0 \sum_{i=1}^{n} a_i \exp(z/\zeta_i)$			
Defant (1961)	Wavelength (μm)	a_i	ζ_i (m)
	0.2–0.6	0.237	34.849
	0.6–0.9	0.360	2.2661
	0.9–1.2	0.179	3.1486×10^{-2}
	1.2–1.5	0.087	5.4831×10^{-3}
	1.5–1.8	0.080	8.3170×10^{-4}
	1.8–2.1	0.0246	1.2612×10^{-4}
	2.1–2.4	0.025	3.1326×10^{-4}
	2.4–2.7	0.007	7.8186×10^{-5}
	2.7–3.0	0.0004	1.4427×10^{-5}
IV [Eq. (5)]			
Arctangent: $I(z) = I_0 \exp(z/\zeta_2)[1 - R \tan^{-1}(-z/\zeta_1)]$		ζ_1	ζ_2
Zaneveld and Spinrad (1980)	R	(m)	(m)
	0.3963	0.22	22.7

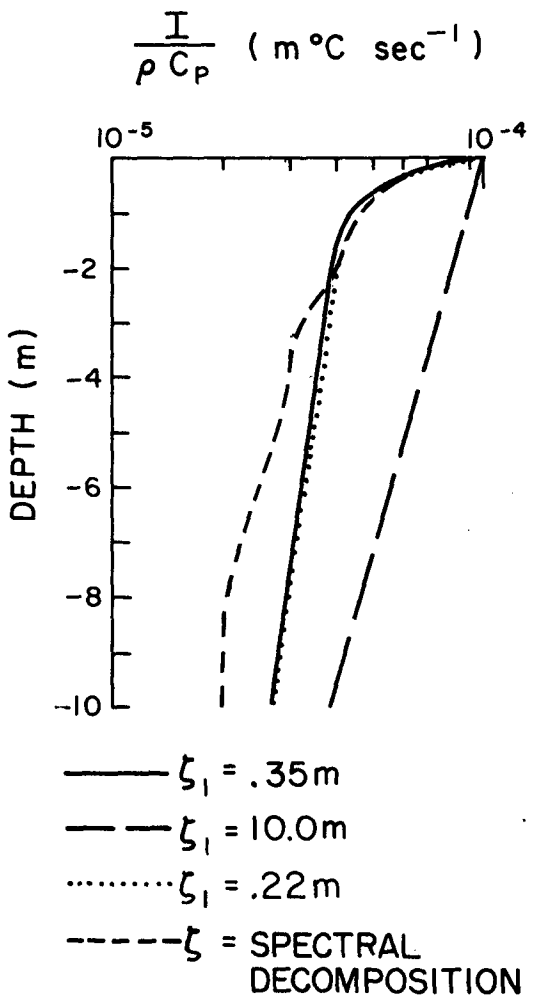

FIG. 2. Vertical profiles of downward irradiance constructed from Eqs. (2) — —, (3) ——, (4) - - - and (5) -----.

optimized with a logarithmic distribution. This is ideal for the input of the penetrative component of solar irradiance. There are 101 levels for the upper 50 m with the density of grid points greatest near the surface. The grid resolution in the interior is ~0.5 m. As a sensitivity test, the number of grid points in this region was varied by a factor of 4 with virtually no effect. The time step was 1 h. Simulations were run for 72 h and the effects of spin-up are observed during the first few hours. The boundary conditions for the model and the conditions common to all runs are given by Simpson and Dickey (1981).

The temperature structure for the low wind speed simulations (U_{10} = 2 m s^{-1}) is shown in Fig. 3 for all parameterizations. The initial profile and subsequent profiles at t = 12, 18 and 24 h are shown. In the following discussion parameterizations based on Eqs. (2)–(5) are referred to as case I through case IV, respectively. The mean temperature structure for cases II–IV is qualitatively quite similar. These three cases show warmer sea surface temperatures, shallower mixed-layer depths, and more intense thermoclines when compared to case I. Quantitative differences among cases II–IV are insignificant. For example, at t = 24 h the predicted sea surface temperatures for these cases are 9.99, 10.08 and 9.99°C, respectively. For each of these cases, the predicted mixed-layer depth, based on a Richardson number criterion (e.g., Mellor and Durbin, 1975), is nearly the same, 0.4 m. However, the corresponding quantities for the case I simulation, 8.68°C and 5.8 m, differ significantly from the other simulations. Even after 72 h, the case II–IV simulations predict sea surface temperatures (13.19, 13.49 and 13.26°, respectively) within a few tenths of a degree of each other. Within this group of cases, the coldest sea surface temperatures are predicted by case II, the bi-modal exponential parameterization, and the warmest by case III, the spectral decomposition parameterization. This result is consistent with the optical absorbance characteristics of Eqs. (2)–(5). At t = 72 h, the predicted sea surface temperature for case I is approximately 4°C colder than the mean sea surface temperature of cases II–IV.

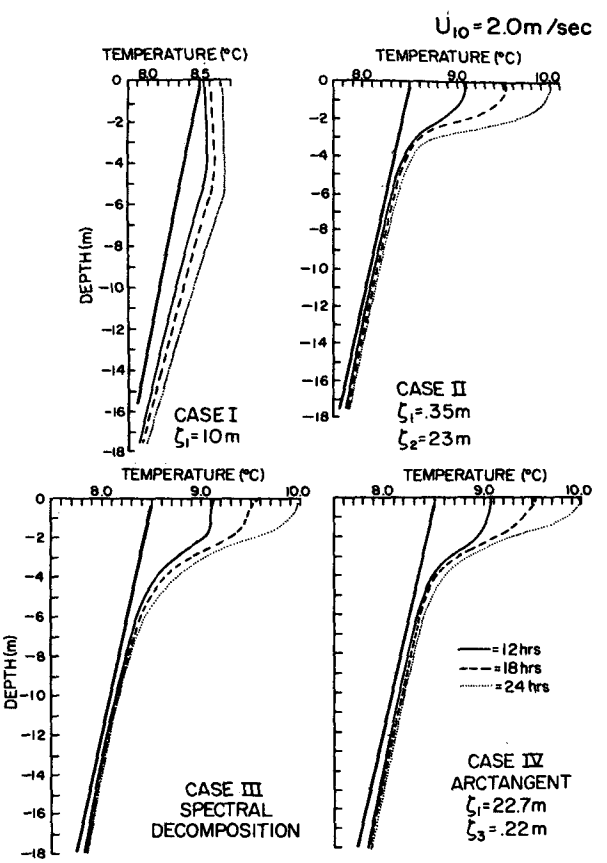

FIG. 3. The initial temperature profile and subsequent profiles at t = 12, 18 and 24 h for all four cases. The wind speed is 2 m s^{-1}.

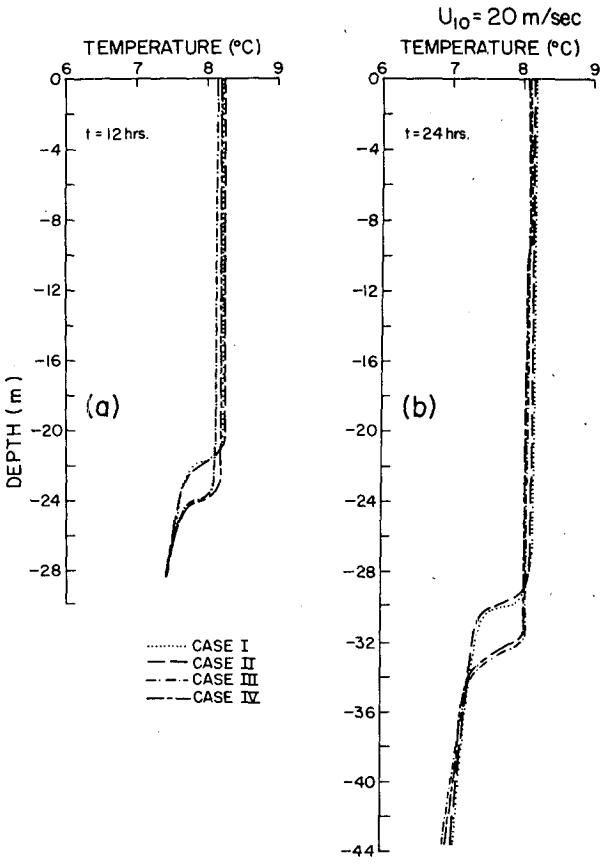

FIG. 4. Temperature profiles at t = 12 and t = 24 h shown for all four cases. The wind speed is 20 m s^{-1}.

Temperature profiles for the high wind speed simulations (U_{10} = 20 m s^{-1}) are shown in Fig. 4. The predicted temperature structure is nearly independent of the parameterization of downward irradiance. For example, at t = 24 h the predicted sea surface temperatures agree to within 0.08°C. The corresponding mixed-layer depths all agree to within a few meters.

Profiles of the mean zonal and meridional velocities after 72 h with a uniform wind speed of 2 m s^{-1} are shown in Figs. 5a and 5b, respectively. Cases II–IV show nearly identical velocity structure. A region of enhanced shear is seen in the near surface layer which extends to an approximate depth of 1 m. This feature may be explained in large part by the highly stratified density profiles (see Fig. 3) which results from case II–IV irradiance parameterizations under low wind speeds. The existence of such an intensified shallow shear zone has been observed recently by Dillon and Richman (1980). Under conditions of low wind speed ($\bar{U}_{10}$ = 4.8 m s^{-1}), small surface waves and summertime heating, they found intense turbulence in the upper 1 m of Green Peter Reservoir. Case I simulations, however, depart significantly from this pattern. Little shear is seen in the velocity profile for case I. The magnitude of the velocity is decreased because the mixed layer is much deeper than for cases II–IV.

Analogous velocity profiles for the high wind speed simulations (U_{10} = 20 m s^{-1}) are shown in Figs. 6a and 6b. Through a depth of approximately 50 m, no appreciable difference is seen in the velocity structure. Below a depth of 50 m (the approximate depth of the mixed layer) there are differences in both the mean zonal and meridional components of velocity. These appear to result from differences in the density structure at the base of the mixed layer.

In an earlier paper, Simpson and Dickey (1981) computed the turbulence energy budget for case I and case II irradiance parameterizations. They found that for low wind speeds the turbulence energy budget was dominated by shear production, dissipation, and the diffusion of turbulent kinetic energy. For high winds, shear production was balanced by dissipation (see Figs. 12 and 13, Simpson and Dickey, 1981). Similar results were obtained for the case III spectral decomposition and case IV arctangent parameterization of downward irradiance.

Simulations were also done for type II and III ocean water. Type III water is characteristic of biologically productive coastal waters. Results, analogous to those reported above for type I water, were obtained.

4. Conclusions

The effects of downward irradiance on upper ocean structure were examined using the Mellor-Yamada turbulence closure scheme (level 2½). Two wind stress conditions and four general classes of irradiance parameterizations were used in the simulations. The first (case I) involved only one atenuation length, the second (case II) involved two attentuation lengths, the third (case III) used a spectral decomposition of the incident solar flux over nine wavelength bands, and the fourth (case IV) used an arctangent model of downward irradiance. The essential difference among the four classes of parameterizations was the vertical distribution of downward irradiance, and hence heat, within the upper ocean. Cases II–IV provided for enhanced absorption of downward irradiance in the upper few meters.

A summary of conclusions concerning the parameterization of downward irradiance is as follows:

1) The single exponential form (case I) appears to be acceptable *only* at very high wind speeds.

2) The spectral decomposition form (case III) requires that many degrees of freedom be specified. Generally, this level of complexity is not required. However, certain wavelength-dependent processes, such as photosynthesis, gas exchange dynamics and

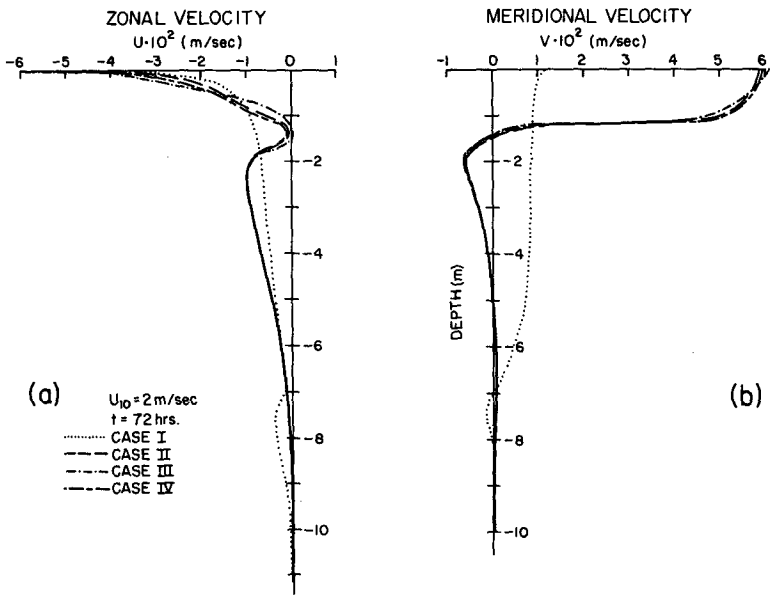

FIG. 5. Profiles of the mean zonal and meridional velocity after 72 h with a uniform wind speed of 2 m s^{-1} for the four different irradiance parameterizations.

thermal boundary layer studies (i.e., Simpson and Paulson, 1980; Woods, 1980; Paulson and Simpson, 1981) may require its use.

3) The bi-modal exponential form (case II) and the arctangent form (case IV) have the same number of degrees of freedom (3), and produce nearly equivalent results.

4) The major differences between the case II and IV parameterizations are:

(i) The length scales ζ_1 and ζ_2 used with the bi-modal exponential are not coupled. Hence, they are easier to interpret physically than the coupled length scales in the arctangent model [i.e., the term $I_0 \exp(z/\zeta_1)R \tan^{-1}(-z/\zeta_2)$].

(ii) Computationally, the bi-modal exponential is somewhat more economical than the arctangent model.

5) Enhanced near-surface absorption is needed for the models to be realistic and any of the irradiance forms II, III and IV are adequate.

Acknowledgments. This research was supported by the Marine Life Research Group of the Scripps Institution of Oceanography and the Department of Geological Sciences and by the Institute for Marine and Coastal Studies of the University of Southern California. Special thanks to Prof. J. L. Reid, Dr. Kern Kenyon and Dr. Ron Zaneveld for a careful review of the preliminary manuscript. Dick Schwartzlose managed to find the resources necessary to com-

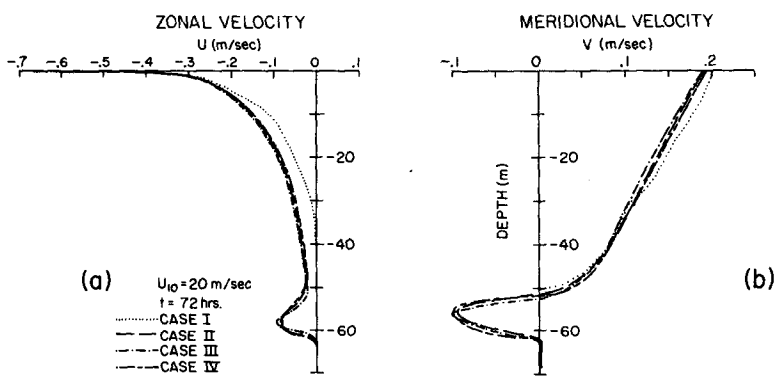

FIG. 6. Velocity profiles, analogous to those in Fig. 5, for a uniform wind speed of 20 m s^{-1}.

plete this task. Bruno Bittner assisted with the computer graphics. Tom Spoering provided the data for Fig. 1. Sharon McBride typed the manuscripts. The figures were prepared by the MLRG Illustrations Group under the able direction of Fred Crowe. Special thanks to my draftsperson in residence, Nancy Hulbirt.

REFERENCES

Alexander, R. C., and J. W. Kim, 1976: Diagnostic model study of mixed layer depths in the summer North Pacific. *J. Phys. Oceanogr.*, **6**, 293–298.

Blumberg, A. F., and G. L. Mellor, 1980: A coastal ocean numerical model. *Mathematical Modelling of Estuarine Physics*, Proceedings of an International Symposium held at the German Hydrographic Institute, Hamburg, August 24–26, 1978, J. Sundermann and K.-P. Holz, Eds., Springer–Verlag, 265 pp. (see pp. 203–219).

Defant, A., 1961: *Physical Oceanography*, Vol. I. Pergamon Press, 729 pp.

Denman, K. L., 1973: A time-dependent model of the upper ocean. *J. Phys. Oceanogr.*, **3**, 173–184.

Dickey, T. D., and J. J. Simpson, 1981: The diurnal response of the upper ocean. Submitted to *J. Phys. Oceanogr.*

Dillon, T. M., and J. G. Richman, 1980: Temperature microstructure in the near-surface layer. *Trans. Amer. Geophys. Union*, **61**, 1005 (abstract).

Garwood, R. W., Jr., 1979: Air-sea interaction and dynamics of the surface mixed layer. *Rev. Geophys. Space Phys.*, **17**, 1507–1524.

Haney, R. L., and R. W. Davies, 1976: The role of surface mixing in the seasonal variation of the ocean thermal structure. *J. Phys. Oceanogr.*, **6**, 504–510.

Jerlov, N. G., 1976: *Marine Optics*. Elsevier, 231 pp.

Kondo, J., Y. Sasano and T. Ishi, 1979: On wind-driven current and temperature profiles with diurnal period in the oceanic planetary boundary layer. *J. Phys. Oceanogr.*, **9**, 360–372.

——, and I. Watabe, 1969: Seasonal changes of vertical profile of water temperature and evaporation from deep lakes (in Japanese with English abstract). *Rep. Nat. Res. Center Disaster Prevention*, **2**, 75–88.

Kraus, E. B., 1972: *Atmosphere-Ocean Interaction*. Clarendon Press, 275 pp.

——, 1977: *Modeling and Predicting of the Upper Layers of the Ocean*. Pergamon Press, 325 pp.

——, and J. S. Turner, 1967: A one-dimensional model of the seasonal thermocline: II. The general theory and its consequences. *Tellus*, **19**, 98–106.

Mellor, G. L., and P. A. Durbin, 1975: The structure and dynamics of the ocean surface layer. *J. Phys. Oceanogr.*, **5**, 718–728.

——, and T. Yamada, 1974: A hierarchy of turbulence closure models for planetary boundary layers. *J. Atmos. Sci.*, **31**, 1791–1806.

Paulson, C. A., and J. J. Simpson, 1977: Irradiance measurements in the upper ocean. *J. Phys. Oceanogr.*, **7**, 952–956.

——, and ——, 1981: The temperature difference across the cool skin of the ocean. Submitted to *J. Geophys. Res.*

Simpson, J. J., and C. A. Paulson, 1980: Small-scale sea surface temperature structure. *J. Phys. Oceanogr.*, **10**, 399–410.

——, and T. D. Dickey, 1981: The relationship between downward irradiance and upper ocean structure. *J. Phys. Oceanogr.*, **11**, 309–323.

Sverdrup, H. U., M. W. Johnson and R. H. Fleming, 1942: *The Oceans: Their Physics, Chemistry and General Biology*. Prentice-Hall, 1087 pp.

Tyler, J. E., and R. W. Preisendorfer, 1962: Transmission of energy within the sea. *The Sea*, Vol. I, M. M. Hill, Ed., Interscience, 397–451.

Woods, J. D., 1980: Diurnal and seasonal variation of convection in the wind-mixed layer of the ocean. *Quart. J. Roy. Meteor. Soc.*, **106**, 379–394.

Yamada, T., 1977: A numerical experiment of pollutant dispersion in a horizontally-homogeneous atmospheric boundary layer. *Atmos. Environ.*, **11**, 1015–1024.

Zaneveld, J. R. V., and R. W. Spinrad, 1980: An arctangent model of irradiance in the sea. *J. Geophys. Res.*, **85**, 4919–4922.